

Shiga-like toxins are neutralized by tailored multivalent carbohydrate ligands

Pavel I. Kitov*, Joanna M. Sadowska*, George Mulvey†, Glen D. Armstrong†, Hong Ling‡, Navraj S. Pannu§, Randy J. Read†‡§ & David R. Bundle*

* Department of Chemistry, University of Alberta, Edmonton, Alberta T6G 2G2, Canada

† Department of Medical Microbiology and Immunology, University of Alberta, Edmonton, Alberta T6G 2H7, Canada

‡ Department of Biochemistry, University of Alberta, Edmonton, Alberta T6G 2H7, Canada

§ Department of Haematology, Cambridge Institute for Medical Research, Wellcome Trust/MRC Building, University of Cambridge, Hills Road, Cambridge CB2 2XY, UK

The diseases caused by Shiga and cholera toxins account for the loss of millions of lives each year¹. Both belong to the clinically significant subset of bacterial AB₅ toxins consisting of an enzymatically active A subunit that gains entry to susceptible mammalian cells after oligosaccharide recognition by the B₅ homopentamer^{2,3}. Therapies might target the obligatory oligosaccharide–toxin recognition event⁴, but the low intrinsic affinity of carbohydrate–protein interactions hampers the development of low-molecular-weight inhibitors⁵. The toxins circumvent low affinity by binding simultaneously to five or more cell-surface carbohydrates⁶. Here we demonstrate the use of the crystal structure of the B₅ subunit of *Escherichia coli* O157:H7 Shiga-like toxin I (SLT-I) in complex with an analogue of its carbohydrate receptor⁶ to design an oligovalent, water-soluble carbohydrate ligand (named STARFISH), with subnanomolar inhibitory activity. The *in vitro* inhibitory activity is 1–10-million-fold higher than that of univalent ligands and is by far the highest molar activity of any inhibitor yet reported for Shiga-like toxins I and II. Crystallography of the STARFISH/Shiga-like toxin I complex explains this activity. Two trisaccharide receptors at the tips of each of five spacer arms simultaneously engage all five B subunits of two toxin molecules.

Shiga toxin, which is produced by *Shigella dysenteriae* type 1, and the homologous Shiga-like toxins (SLTs) of *E. coli*, also called Verotoxins (VTs), can cause serious clinical complications in

humans infected by these organisms^{7–9}. The functional toxin receptor on mammalian cells is the glycolipid Gb₃ (α-D-Gal(1 → 4)β-D-Gal(1 → 4)β-D-Glc(1 → O-ceramide)⁸ and the high incidence of complications such as acute kidney failure in children correlates with the expression of Gb₃ in the paediatric renal glomerulus¹⁰. Synthetic Gb₃ analogues covalently attached to insoluble silica particles competitively adsorb toxin from the gut and the adsorbent Synsorb P^k is currently undergoing clinical trials¹¹. Once the toxin has exited the gut and entered the circulation, however, there is no viable toxin therapy.

Shiga-like toxins from *E. coli* represent a family of structurally and functionally related toxins, which can be classified into two subgroups, SLT-I and SLT-II, on the basis of their relatedness to the prototypic Shiga toxin expressed by *S. dysenteriae*^{12,13}. Nevertheless, homology modelling suggests that structural changes in the binding sites are fairly conservative.

The crystal structure of the SLT-I B-subunit pentamer in complex with a Gb₃ trisaccharide analogue has been solved at 2.8 Å resolution⁶. Three saccharide-binding sites are found in each relative molecular mass 7,700 (M_r 7.7K) subunit. The subunits associate non-covalently to form a doughnut-shaped B-subunit pentamer with 15 saccharide-binding sites aligned on one face of the toxin. The A subunit is attached to the opposite surface of the

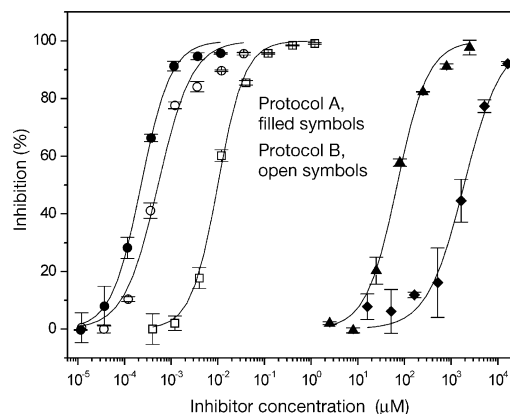


Figure 2 Inhibitor activity by enzyme linked immunosorbent assay (ELISA). Protocol A: diamonds, P^k trisaccharide 1 and SLT-I assay (IC₅₀ = 2.1 mM); triangles, bridged P^k dimer 2 and SLT-I assay (IC₅₀ = 55 μM); solid circles, STARFISH 3 and SLT-I assay (IC₅₀ = 0.24 nM). Protocol B: open circles, STARFISH 3 and SLT-I assay (IC₅₀ = 0.4 nM); open squares, STARFISH 3 and SLT-II assay (IC₅₀ = 6 nM).

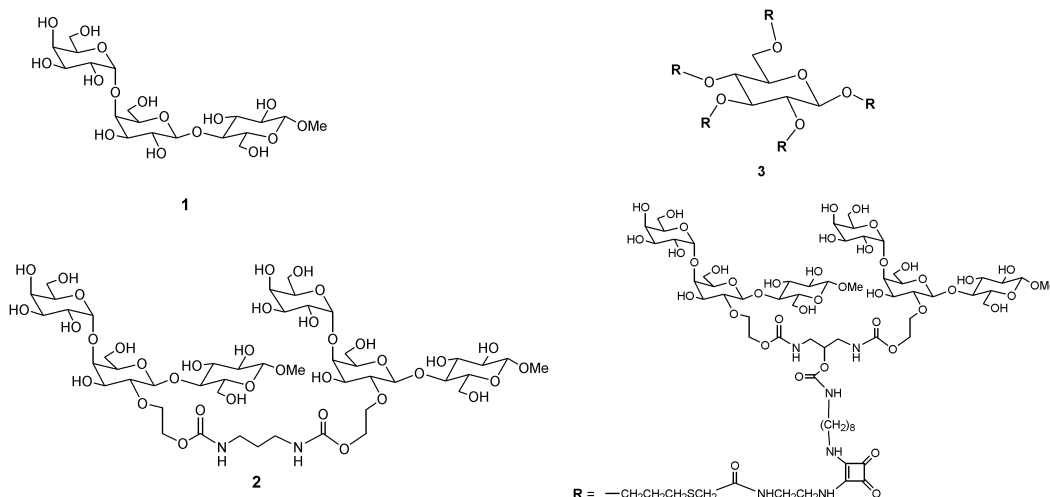


Figure 1 Structures of monomeric and oligomeric P^k inhibitors of Shiga-like toxins. 1, P^k trisaccharide methyl glycoside; 2, dimeric bridged P^k trisaccharide; 3, decameric STARFISH.

B-subunit pentamer^{2,14} thereby allowing all 15 sites to engage cell-surface receptors.

The free energy of binding for the interaction of the B-subunit pentamer with the methyl glycoside of the P^k trisaccharide (compound 1, Fig. 1) is a modest 3.6 kcal mol⁻¹ corresponding to a millimolar dissociation constant (K_d)¹⁵. Functional group modifications of the oligosaccharide's hydroxyl groups showed no substantial gain in binding energy¹⁶, and further investigation of synthetic modifications convinced us that design of a univalent inhibitor based upon functional group modification was unlikely to provide significant affinity increases. 'Random' multivalency of the type seen in acrylamide polymers or in dendrimers has rarely raised lectin-sugar avidity more than 1,000-fold, and the underlying reasons for activity gains of this magnitude are poorly understood³. This approach seemed unlikely to provide the 9–10 kcal mol⁻¹ of free energy required to create a SLT inhibitor with nanomolar activity.

Oligovalency 'tailored' to the structure of the B-subunit pentamer offered the best opportunity to design higher-affinity inhibitors, as 15 binding sites are arranged symmetrically across the toxin surface that engages the cell membrane. Binding and cytotoxicity studies on site-directed mutants suggest that the two peripheral binding sites, 1 and 2, are more important than site 3, which is close to the centre of the pentamer. The most striking effects are observed with a site 2 mutant¹⁷. An NMR structure of SLT-I with and without bound ligand determined that site 2 was the most important binding site for soluble trisaccharide¹⁸. We designed a tethered divalent ligand

that could occupy sites 1 and 2 of a single B subunit and perhaps also increase affinity through fortuitous tether-protein contacts. We found the optimum point for tethering ligands that occupy these sites by examining the crystal structure of the bound ligands in each site. Although hydrogen bonds between the protein and sugar hydroxyl groups are numerous, the orientation of the P^k trisaccharide in both sites exposes the hydroxyl group at the C2 position of the central β -galactose residue to solvent and away from the protein surface. At their closest point of separation, the O2' atoms of the Gb₃ ligands in sites 1 and 2 are separated by 9–10 Å. The synthetic assembly of two P^k ligands tethered at the same attachment point, therefore, offered a synthetically conservative approach to a divalent ligand. A simple synthetic route was designed to create a tethered dimer of P^k trisaccharides (compound 2, Fig. 1).

In assays to measure the ability of inhibitors to block binding of a biotin-labelled P^k-BSA (bovine serum albumin) glycoconjugate to SLT-I, compound 2, a bridged P^k trisaccharide dimer (Fig. 2), reached a K_d of 10⁻⁵ M. Although 40-fold higher than the univalent P^k trisaccharide 1, the dimer activity compares poorly with the estimated affinity ($K_d = 10^{-9}$ M) of the B-subunit pentamer for cells that express Gb₃ (ref. 19).

However, this bridged P^k dimer could be used in an optimally tailored pentameric cluster that could embrace the entire toxin surface and provide sufficient ligand copies to saturate all the important binding sites. Building tethers of appropriate lengths between distinct bridged carbohydrate dimers that could reside in binding sites 1 and 2 of B-subunit monomers would result in a

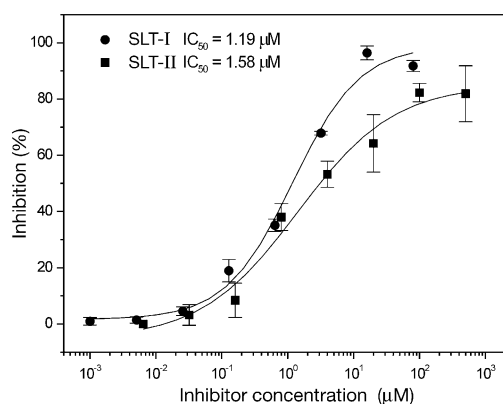


Figure 3 Cytotoxicity assay. Vero cells were incubated with synthetic inhibitors and an otherwise lethal dose of SLT-I or SLT-II. Assays of STARFISH 3 with SLT-I (filled circles) and SLT-II (filled squares).

Table 1 Crystallographic data

Space group	C2
Unit cell	$a = 104.47 \text{ \AA}, b = 71.61 \text{ \AA}, c = 56.36 \text{ \AA}, \beta = 109.0^\circ$
Resolution	2.23 Å
Number of reflections	19,159
R_{meas}	
Overall	16.1%
Highest resolution bin	33.9% (2.23–2.34 Å)
Data completeness	
Overall	99.0%
Highest resolution bin	94.9% (2.23–2.34 Å)
Number of non-hydrogen atoms	
Protein	2,700
STARFISH	240
Solvent	80
R factor	17.1%
R_{free}	18.4%
R.m.s. deviation bond angles	1.251°
R.m.s. deviation bond lengths	0.091 Å

* R_{free} set was selected in shells and consisted of 1064 reflections.

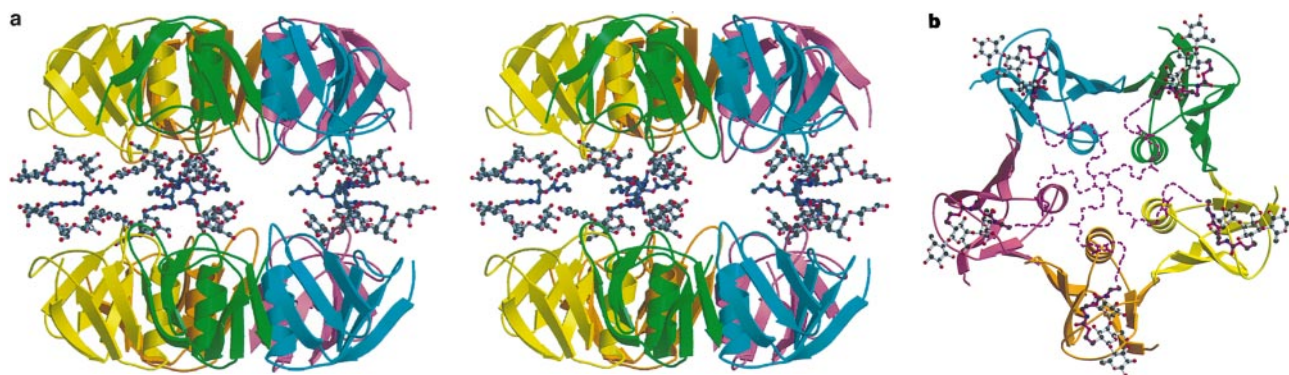


Figure 4 Mode of binding in the STARFISH-SLT-1 complex. **a**, Stereo diagram of the crystallographic dimer of B-subunit pentamers of SLT-I linked by the STARFISH ligand. For the protein, β -strands are illustrated as broad arrows and α -helices as coiled ribbons. The ligand is shown in a ball-and-stick representation, with grey bonds connecting atoms of the carbohydrate component and magenta bonds connecting atoms of the linker.

b, Diagram of half of the STARFISH:SLT-1 B₅ sandwich. The representation is as in **a**, except that dashed magenta lines show a possible conformation for the central component of the linker, which could not be seen clearly in the electron density. These figures were drawn with MolScript²⁹ and rendered with Raster3D³⁰.

multivalent inhibitor that should produce significant avidity gains through entropic savings. Because the peripheral trisaccharides are closer to each other ($\sim 10 \text{ \AA}$) than their respective spacing from the centre of the pentameric complex ($\sim 30 \text{ \AA}$), they can be tethered together and then the dimers assembled into a five-ray cluster (Fig. 1).

We reasoned that pentameric display of P^k trisaccharides at the tips of five appropriately oriented arms that radiate from a central core would allow all five bridged P^k dimers to be simultaneously engaged by the B-subunit pentamer in much the same way that the membrane surface binds toxin. To achieve this display of tethered ligands, a glucose molecule was chosen as the central core²⁰. By derivatizing the glucose as a penta-allyl ether, free-radical reaction with thioglycolic acid was possible and subsequent chain elongation of the radial arms could be achieved by simple uniform chemistry that allowed rapid assembly. Each arm was designed to span the $\sim 30 \text{ \AA}$ from the central pore of the toxin and the tether was designed to bridge binding sites 1 and 2 on each B subunit. The resulting molecule resembles a starfish and hence is named STARFISH (compound 3, Fig. 1).

STARFISH exhibited more than a million-fold increase in inhibition over P^k trisaccharide 1. This subnanomolar activity lies within the range desired for an anti-adhesive therapeutic. Owing to the assay format and lower intrinsic affinities of the SLT-II binding sites, this activity could be measured for SLT-I but not for SLT-II. Protocol A (Fig. 2) uses toxin adsorbed to microtitre plates, and adsorbed SLT-II did not give a signal with the P^k -BSA glycoconjugate reporter molecule because the lower intrinsic affinities of the SLT-II binding sites result in a short half-life of the bound enzyme-linked immunosorbent assay (ELISA) reporter molecule which dissociates from the plate during the multiple washing steps.

To assay SLT-II binding, we developed a solid-phase inhibition assay that allowed the comparison of SLT-I and SLT-II in a single assay format (protocol B, Fig. 2). A synthetic P^k -like glycolipid, developed for detecting SLTs with a biosensor²¹, was used as the solid-phase capture ligand, and bound toxin was detected by a toxin-specific antibody. In this format, both SLT-I and SLT-II bound to the plate with SLT-II showing ~ 10 -fold weaker avidity for the immobilized ligand. Again, the STARFISH inhibitor had a half-maximal inhibitory concentration (IC_{50}) of $4 \times 10^{-10} \text{ M}$ with SLT-I, but also had an IC_{50} of $6 \times 10^{-9} \text{ M}$ with SLT-II (Fig. 2). The assay thus confirmed that the ligand for SLT-II is the P^k trisaccharide.

The ability of inhibitors to protect host cells against a lethal dose of SLT-I in culture can be determined using Vero cells¹¹. STARFISH inhibitor provided effective protection of Vero cells cultured in the presence of SLT-I and SLT-II, even over the 2-day co-incubation period (Fig. 3).

Crystallographic study of the complex formed between the B-subunit pentamer of SLT-I and STARFISH revealed a mode of binding that differs from the one originally envisaged by 'rational design'. The crystal structure shows that one STARFISH molecule binds to not one but two B-subunit pentamers (Fig. 4). Instead of bridging sites 1 and 2, the tethered P^k trisaccharides of STARFISH bind to two B-subunit monomers from separate toxin molecules. The two B-subunit pentamers are related by a crystallographic twofold axis that passes through the pseudo-twofold symmetric STARFISH molecules, and only site 2 is occupied in all the B-subunit monomers. The trisaccharide is well ordered (mean B -factors: α -galactose residues, 21.5 \AA^2 ; β -galactose residues, 28.9 \AA^2 ; glucose residues, 43.6 \AA^2), its binding interactions are identical to those seen for the univalent ligand⁶, and STARFISH binding does not perturb the protein. As, in this experiment, the concentration of STARFISH was sufficient to form a 1:1 complex, the formation of the 2:1 sandwich must be thermodynamically favoured. Table 1 gives a summary of the crystallographic statistics. The design elements that target the inhibitor to embrace the toxin surface clearly succeeded in placing the P^k trisaccharides in each B subunit.

However, the bivalent ligand at the end of each arm occupies only site 2 of a single B subunit and does not bridge sites 1 and 2 as planned. This results in an unexpected benefit as each arm now presents an unbound P^k trisaccharide and these five epitopes are fortuitously spaced to bind across the face of a second toxin molecule. This interaction is favoured over intramolecular bridging of sites 1 and 2, owing presumably to the previously reported higher affinity of binding site 2 and perhaps also to potential strain in the bridge.

The high inhibitory activity of a multivalent cluster tailored to complement the distribution of oligosaccharide-binding sites across the toxin surface is unusual for glycoconjugates of such size and modest valency. The efficacy of this particular design might be improved by decreasing the entropic penalty through the use of more rigid spacers that link the distal epitopes to the central core. Perhaps the most important feature of this design is the use of dimers that bridge two toxin molecules. Intriguingly, the formation of a toxin dimer indicates that the general inhibitor design may be applicable to other bacterial AB_5 toxins such as cholera toxin or heat-labile enterotoxin. Specific complexation of STARFISH with site 2 of SLT-I, which also possesses the highest affinity in solution^{17,18}, is significant as the single sugar-binding site per B subunit that is found in cholera and heat-labile toxins² corresponds topologically to site 2 of SLT⁶. Hence, the STARFISH bridged-dimer design feature may be general and capable of extension to cholera toxin and heat-labile toxin. In such cases, where each B subunit contains only one sugar-binding site, the ability to bridge between toxin molecules would be essential to achieve potent inhibitory activity.

We have shown that the STARFISH inhibitor protects susceptible cells against prolonged exposure not only to SLT-I but also to the reportedly more clinically significant SLT-II (ref. 22), a toxin for which there were previously no inhibitors. In view of their potent activity, these inhibitors represent a potential treatment for preventing kidney damage that occurs after serious cases of toxin poisoning. This confirms the potential of carbohydrates as new and viable bacterial anti-adhesive therapeutics, which was first suggested by Sharon and co-workers⁴ some 20 years ago. \square

Methods

Inhibitors

The inhibitors were synthesized by methods that will be published elsewhere. We characterized them by elemental analysis, NMR, and MALDI (matrix-assisted laser desorption/ionization), electrospray and ion cyclotron resonance mass spectrometry to confirm their structures. Shiga-like toxins I and II were purified according to published methods²³.

Solid-phase binding assays

Protocol A: SLT-I dissolved in PBS (100 μl ; $2.5 \mu\text{g ml}^{-1}$) was coated on 96-well ELISA plates (18 h at 4°C). The plate was washed five times with PBST (PBS containing Tween 20, 0.05% v/v), blocked for 1 h with milk (DIFCO, 2.5% in PBS, 100 μl). The plate was washed twice with PBST. A P^k trisaccharide conjugated to BSA and biotinylated ($10 \mu\text{g ml}^{-1}$) was mixed with inhibitor at concentrations in the range 0.1 nM to 10 mM, and the mixture (100 μl) was added to the coated microtitre plate and incubated at room temperature (18 h). The plate was washed five times with PBST and streptavidin horseradish peroxidase conjugate (100 μl) was added and incubated for 1 h at room temperature. The plate was washed five times with PBST, 3,3',5,5'-tetramethylbenzidine (TMB, 100 μl) was added, and after 2 min the colour reaction was stopped by the addition of 1 M phosphoric acid (100 μl). Absorbance was measured at 450 nm and the percentage inhibition was calculated using wells containing no inhibitor as the reference point.

Protocol B: a synthetic P^k trisaccharide attached to a C_{16} aglycon terminated by an ω -thiol and oxidized to the corresponding disulphide 4 (ref. 22) was dissolved in PBS (10 $\mu\text{g ml}^{-1}$), and coated on 96-well ELISA plates (100 μl , 18 h at 4°C). The plate was washed five times with PBST and blocked for 1 h at room temperature by incubation with 1% BSA in PBS (100 μl). The plate was washed three times with PBST, and SLT solution (100 μl) was added to the plate (SLT-I at $0.05 \mu\text{g ml}^{-1}$ or SLT-II at $0.1 \mu\text{g ml}^{-1}$). The SLT solution with or without inhibitor was incubated for 18 h at room temperature. The plate was washed five times with PBST, and rabbit anti-SLT-I or SLT-II solution (100 μl) diluted in PBS (1:1000) was incubated for 1 h at room temperature. After the plate had been washed five times with PBST, commercial horseradish-peroxidase-labelled, goat anti-rabbit antibody solution (100 μl) diluted (1:2000) in PBS was incubated for 1 h at room temperature. The plate was washed five times with PBST, and colour was developed and measured as described in protocol A.

Cytotoxicity assay^{11,23}

STARFISH inhibitor was dissolved in double-distilled, deionized water. Stock solutions of purified SLT-I and SLT-II were prepared at concentrations of 400 ng ml⁻¹ and 2 µg ml⁻¹, respectively, in unsupplemented MEM. Serial dilutions, in unsupplemented MEM, of inhibitor solution were prepared using a 96-well microtitre plate. Next, 5 µl of stock SLT-I or SLT-II solution was added to each well (to 80 µl final volume) of the appropriate rows in the dilution plate. The solution in each of the dilution plate wells was thoroughly mixed and the microtitre plate was incubated for 1 h at 37 °C, after which 20 µl from each well was transferred to the corresponding well of a 96-well microtitre plate containing confluent Vero cell monolayers and 200 µl of MEM supplemented with fetal bovine serum. The Vero cell microtitre plate was incubated for an additional 48 h in a 37 °C incubator in an atmosphere of 5% CO₂/95% air. The Vero cell monolayers were then fixed with methanol and cytotoxicity was measured as described¹¹.

Crystallography

A solution of the complex was made by adding 15 µl of a solution of STARFISH (0.35 mM in water) slowly to 15 µl of SLT-I B subunit (10 mg ml⁻¹, 0.1 M NaCl and 10 mM Tris pH 8.0) with agitation. We mixed this solution with an equal volume of reservoir solution (28% saturated ammonium sulfate, 2% 2-methyl-2,4-pentanediol, 0.1 M NaCl and 0.1 M Hepes pH 7.0) for hanging drops. Crystals grew at room temperature as clusters of needles. Diffraction data, collected on a MAR345 detector mounted on a Rigaku rotating anode generator, extended to 2.23 Å resolution (Table 1). A molecular replacement solution was obtained in AMoRe²⁴ using the B subunit of the crystal structure of the SLT-I B-subunit pentamer complexed with Gb₃ (ref. 6) as a model. The test set was selected in thin shells to limit the bias that may be introduced by the fivefold non-crystallographic symmetry (NCS) present in the asymmetric unit. Refinement was carried out in CNS²⁵ using maximum-likelihood targets²⁶, and strict NCS followed by restrained NCS. Manual intervention in between cycles of refinement using the XTALVIEW package²⁷ and averaged cross-validated SigmaA²⁸ maps allowed the building of part of the STARFISH molecule. The STARFISH molecule is fully occupied in the crystal, but, because of symmetry, parts of the linker are only half occupied in the crystallographic asymmetric unit.

Received 1 September; accepted 30 November 1999.

- Holmgren, J. & Svennerholm, A. M. Bacterial enteric infections and vaccine development. *Gastroenterology Clinics of North America* **21**, 283–302 (1992).
- Merritt, E. A. & Hol, W. G. J. AB₅ toxins. *Curr. Opin. Struct. Biol.* **5**, 165–171 (1995).
- Lindberg, A. A. *et al.* Identification of the carbohydrate receptor for Shiga toxin produced by *Shigella dysenteriae* Type 1. *J. Biol. Chem.* **262**, 1779–1785 (1987).
- Aronson, M. *et al.* Prevention of colonization of the urinary tract of mice with *Escherichia coli* by blocking of bacterial adherence with methyl α-D-mannopyranoside. *J. Infect. Dis.* **139**, 329–332 (1979).
- Mammen, M., Choi, S.-K. & Whitesides, G. M. Polyvalent interactions in biological systems: implications for design and use of multivalent ligands and inhibitors. *Angew. Chem. Int. Ed.* **37**, 2754 (1998).
- Ling, H. *et al.* Structure of the Shiga-like toxin I B-pentamer complexed with an analogue of its receptor Gb₃. *Biochemistry* **37**, 1777–1788 (1998).
- Karmali, M. A., Steele, B. T., Petric, M. & Lim, C. Sporadic cases of haemolytic-uremic syndrome associated with fecal cytotoxin and cytotoxin-producing *Escherichia coli* in stools. *Lancet* **i**, 619–620 (1983).
- Karmali, M. A. *et al.* The association between idiopathic hemolytic uremic syndrome and infection by Verotoxin-producing *Escherichia coli*. *J. Infect. Dis.* **151**, 775–782 (1985).
- Cimolai, N., Carter, J. E., Morrison, B. J. & Anderson, J. D. Risk factors for the progression of *Escherichia coli* O 157:H7 enteritis to hemolytic-uremic syndrome. *J. Pediatr.* **116**, 589–592 (1990).
- Boyd, B. & Lingwood, C. Verotoxin receptor glycolipid in human renal tissue. *Nephron* **51**, 207–210 (1989).
- Armstrong, G. D., Fodor, E. & Vanmaele, R. Investigation of Shiga-like toxin binding to chemically synthesized oligosaccharide sequences. *J. Infect. Dis.* **164**, 1160–1167 (1991).
- O'Brien, A. D. *et al.* Shiga toxin: biochemistry, genetics, mode of action, and role in pathogenesis. *Curr. Top. Microbiol. Immunol.* **180**, 65–94 (1992).
- DeGrandis, S. *et al.* Nucleotide sequence and promoter mapping of the *Escherichia coli* Shiga-like toxin operon of bacteriophage H-19B. *J. Bacteriol.* **169**, 4313–4319 (1987).
- Stein, P. E., Boodhoo, A., Tyrrell, G. J., Brunton, J. L. & Read, R. J. Crystal structure of the cell-binding B oligomer of verotoxin-1 from *E. coli*. *Nature* **355**, 748–750 (1992).
- St. Hilaire, P. M., Boyd, M. K. & Toone, E. J. Interaction of the Shiga-like type 1 B-subunit with its carbohydrate receptor. *Biochemistry* **33**, 14452–14463 (1994).
- Nyholm, P. G. *et al.* Two distinct binding sites for globotriaosyl on verotoxins: identification by molecular modelling and confirmation using deoxy analogues and a new glycolipid receptor for all verotoxins. *Chem. Biol.* **3**, 263–275 (1996).
- Bast, D. J., Banerjee, L., Clark, C., Read, R. J. & Brunton, J. L. The identification of three biologically relevant globotriaosyl ceramide receptor binding sites on the Verotoxin 1 B subunit. *Mol. Microbiol.* **32**, 953–960 (1999).
- Shimizu, H., Field, R. A., Homans, S. W. & Donohue-Rolfé, A. Solution structure of the complex between the B-subunit homopentamer of verotoxin VT-1 from *Escherichia coli* and the trisaccharide moiety of globotriaosylceramide. *Biochemistry* **31**, 11078–11082 (1998).
- Fuchs, G. *et al.* Pathogenesis of *Shigella* diarrhea: rabbit intestinal cell microvillus membrane binding site for *Shigella* toxin. *Infect. Immun.* **53**, 372–377 (1986).
- Dubber, M. & Lindhorst, T. K. Synthesis of octopus glycosides: core molecules for the construction of glycoclusters and carbohydrate-centered dendrimers. *Carbohydr. Res.* **310**, 35–41 (1998).
- Kitov, P. I., Raiton, C. & Bundle, D. R. The synthesis of 16-mercaptopentadecanyl glycosides for biosensor applications. *Carbohydr. Res.* **307**, 361–369 (1998).
- Tesh, V. L. *et al.* Comparison of the relative toxicities of Shiga-like toxins type I and type II for mice. *Infect. Immun.* **61**, 3392–3402 (1993).

- Mulvey, G., Vanmaele, R., Mrazek, M., Cahill, M. & Armstrong, G. D. Affinity purification of Shiga-like toxin I and Shiga-like toxin II. *J. Microbiol. Methods* **32**, 247–252 (1998).
- Navaza, J. AMoRe: an automated package for molecular replacement. *Acta Crystallogr. A* **50**, 157–163 (1994).
- Brünger, A. T. *et al.* Crystallography & NMR system: a new software suite for macromolecular structure determination. *Acta Crystallogr. D* **54**, 905–921 (1998).
- Pannu, N. S. & Read, R. J. Improved structure refinement through maximum likelihood. *Acta Crystallogr. A* **52**, 659–668 (1996).
- McRee, D. E. XtalView/Xfit—a versatile program for manipulating atomic coordinates and electron density. *J. Struct. Biol.* **125**, 156–165 (1999).
- Read, R. J. Model phases: probabilities and bias. *Methods Enzymol.* **277**, 110–128 (1997).
- Kraulis, P. J. MOLSCRIPT: a program to produce both detailed and schematic plots of protein structures. *J. Appl. Crystallogr.* **24**, 946–950 (1991).
- Merritt, E. A. & Bacon, D. J. Raster3D: photorealistic molecular graphics. *Methods Enzymol.* **277**, 505–524 (1997).

Acknowledgements

Protein used in the crystallographic experiments was a generous gift from J. L. Brunton. This work was supported by grants from the Canadian Bacterial Disease Network and a grant to R.J.R. from the Wellcome Trust (UK). We thank the MRC Laboratory of Molecular Biology in Cambridge for the allocation of resources for diffraction data collection, B. Hazes for assistance in data collection, and K. Hayakawa for technical assistance in growing the crystals.

Correspondence and requests for materials should be addressed to D.R.B. Coordinates and structure factors have been deposited in the Protein Data Bank under accession code 1qnu.

How self-tolerance and the immunosuppressive drug FK506 prevent B-cell mitogenesis

Richard Glynn^{*†}, Srinivas Akkaraju^{*}, James I. Healy^{*}, Jane Rayner[‡], Christopher C. Goodnow^{*‡} & David H. Mack[§]

^{*} Department of Microbiology and Immunology, Beckman Center, Stanford University, Stanford, California 94305, USA

[‡] Medical Genome Centre, John Curtin School of Medical Research, Australian National University, Canberra 2601, Australia

[§] Eos Biotechnology, 225A Gateway Boulevard, South San Francisco, California 94080, USA

Therapy for transplant rejection, autoimmune disease and allergy must target mature lymphocytes that have escaped censoring during their development. FK506 and cyclosporin are immunosuppressants which block three antigen-receptor signalling pathways (NFAT, NFκB and JNK), through inhibition of calcineurin¹, and inhibit mature lymphocyte proliferation to antigen^{2–4}. Neither drug induces long-lived tolerance *in vivo*, however, necessitating chronic use with adverse side effects. Physiological mechanisms of peripheral tolerance to self-antigens provide an opportunity to emulate these processes pharmacologically. Here we use gene-expression arrays to provide a molecular explanation for the loss of mitogenic response in peripheral B-cell anergy, one aspect of immunological tolerance⁵. Self-antigen induces a set of genes that includes negative regulators of signalling and transcription but not genes that promote proliferation. FK506 interferes with calcium-dependent components of the tolerance response and blocks an unexpectedly small fraction of the activation response. Many genes that were not previously connected to self-tolerance are revealed, and our findings provide a molecular fingerprint for the development of improved immunosuppressants that prevent lymphocyte activation without blocking peripheral tolerance.

[†] Present address: Eos Biotechnology, 225A Gateway Boulevard, South San Francisco, California 94080, USA.